Benzina et al., J Material Sci Eng 2016, 5:3
DOI: 10.4172/2169-0022.1000238

Journal of Material Science & Engineering

Research Article Open Access

Translational Development of Biocompatible X-Ray Visible Microspheres for Use in Transcatheter Embolization Procedures

Benzina A[1], Aldenhoff YB[2], Heijboer R[3] and Koole LH[2,4]*

[1]*Faculty of Health, Medicine and Life Sciences, Maastricht University, UniSingel 50, 6229 ER Maastricht, The Netherlands*
[2]*Interface Biomaterials BV, B. Lemmensstraat 364, 6163 JT Geleen, The Netherlands*
[3]*Zuyderland Medisch Centrum, Henri Dunantstraat 5, 6419 PC Heerlen, The Netherlands*
[4]*Department of Biomedical Engineering, University of Malaya, Jalan Universiti, 50603 Kuala Lumpur, Malaysia*

Abstract

Embolization is a minimally invasive treatment that specifically blocks the arterial blood flow into a target blood vessel bed, which is usually a benign or malignant tumor. The aim of the procedure is to shrink the tumor and/or to retard its growth. Embolization the injection of embolic particles via a catheter tube, of which the tip has been navigated carefully (under X-ray guidance) into an arterial branch that exclusively feeds the tumor, and no surrounding healthy tissues. Most of the clinical experience with embolization relates to treatment of leiomyomata (benign tumors growing in the wall of the uterus). There is solid evidence that catheter-based embolization of leiomyomata provides a fully acceptable therapeutic alternative for much more demanding surgical procedures (i.e., hysterectomy and myomectomy). Embolization offers much faster recovery, possible options to become pregnant, and considerable cost saving. There are several commercial brands of embolization agents, suitable to treat leiomyomata. We hypothesized, some years ago, that these products are suboptimal, and that embolization of leiomyomata may be improved further through better engineering of the embolic particles. We developed injectable radiopaque polymer microspheres, which can be monitored during and after the embolization procedure. The embolic microbeads are X-ray traceable, and this has been achieved without compromising other essential properties, such as structural stability and excellent biocompatibility. Herein, we describe new the features of the new embolic microspheres, as observed in preclinical experiments and in the first clinical cases. It is mentioned briefly that this work became an example of successful translation: it has led to a new medical device (Class-IIB) that is now CE-certified and commercially available throughout Europe.

Keywords: Embolization; Radiopacity; X-ray visibility; Polymer microspheres

Introduction

The hallmark of minimally invasive therapy is the endovascular coronary stent, which secures that a coronary atherosclerotic lesion remains open after percutaneous translumenal angioplasty [1]. Stenting has become the preferred revascularization modality in patients with coronary single-vessel or low-risk multivessel disease. The technique is minimally invasive, fast, relatively cheap, and associated with faster patient recovery. Over the years, coronary stenting has seen many technical improvements, in part due to the exploitation of improved biomaterials [2,3]. Recently this has culminated in the development of polymer bio-eroding and drug-eluting vascular scaffolds [4,5].

During the last years, comparable minimally invasive techniques have gained importance in other fields as well. An important example is found in gynaecology, particularly in the treatment of benign tumors that grow in the uterus wall (leiomyomata) [6]. This disease, too, can be treated effectively in a minimally invasive manner, i.e. through controlled targeted injection of embolic particles (diameter around 500 μm) into the arterial vessel tree of each fibroid, via a catheter tube [7-10]. The particles are usually spherical (microspheres), but they can also be irregular [11]. The procedure is known as TACE (TransArterial ChemoEmbolization), and is performed by an interventional radiologist. Embolization is carried out under real-time X-ray fluoroscopic guidance in a dedicated angiosuite, which is comparable to the facility that is used for coronary stenting. There is good evidence that embolization of leiomyomata provides a genuine alternative for the two surgical techniques which are used classically: myomectomy (which is not always possible, depending on shape and location of the myomas), and hysterectomy (which involves radical excision of the uterus and all benign tumors growing therein) [12-15]. Embolization offers significant advantages in terms of patient comfort, and recovery is fast. Psychological burden, which is inevitably associated with hysterectomy, can largely be avoided. Several cases of pregnancy after embolization of leiomyomata have been reported [16,17], but the actual fertility rate after this treatment is still uncertain [18].

It is important to underline that embolization is also rapidly gaining importance in the treatment of malignant tumors, particularly those in the liver or in the kidney. However, embolization of malignant tumors usually stimulates angiogenesis, leading to the formation of new arteries guiding the arterial blood around the embolic obstacles. Hence, embolization of malignant tumors must be accompanied by local or systemic chemotherapy.

Our interest in embolization started when we realized that chemical synthesis in the context of (bio)materials science offers possibilities to add functionalities to the injectable embolizing particles. We (and others) hypothesized that efficacy and safety of TACE for the treatment of leiomyomata can be enhanced when the embolic microspheres would

***Corresponding author:** Koole LH, Interface Biomaterials BV, B. Lemmensstraat 364, 6163 JT Geleen, The Netherlands, Tel: 31464757989; E-mail: koole.leo@gmail.com

Received February 02, 2016; **Accepted** March 04, 2016; **Published** March 14, 2016

Citation: Benzina A, Aldenhoff YB, Heijboer R, Koole LH (2016) Translational Development of Biocompatible X-Ray Visible Microspheres for Use in Transcatheter Embolization Procedures. J Material Sci Eng 5: 238. doi:10.4172/2169-0022.1000238

be radiopaque (i.e. detectable via X-ray fluoroscopy) [19-26]. Note that X-ray fluoroscopy is used in every procedure anyway, for roadmapping during navigation of the catheter's tip, and also to determine the procedure's end point. Note, furthermore, that all existing commercial products for embolization use embolic particles that consist of classical polymers (such as polyvinyl alcohol), which are radiolucent [24]. We reasoned that use of radiopaque microspheres will enable interventional radiologists to actually monitor the synthetic emboli *in situ*. We discussed this idea extensively with >20 interventionalists/TACE experts, and found broad consensus that this feature would help to enhance accuracy and safety of targeted embolization. According to recent literature, the idea is rapidly gaining acceptance [23-26]. Previously, we have described the preparation of our radiopaque microspheres, of which the key elements can be summarized as follows [20]:

- Only reactive monomers belonging to the methacrylate family are used. Linear and crosslinked poly (methacrylate)s are widely used in permanent implants (bone cements, intraocular lenses), and these materials are well-known for their long-term biocompatibility and stability.
- Microspheres are manufactured through suspension polymerization. Subsequently, the particles are size-sorted through automated sieving.
- Radiopacity is introduced through the use of a methacrylate monomer that contains covalently bound iodine (Figure 1a), and hydrophilicity is introduced through use of the monomer 2-hydroxy-ethylmethacrylate (HEMA).

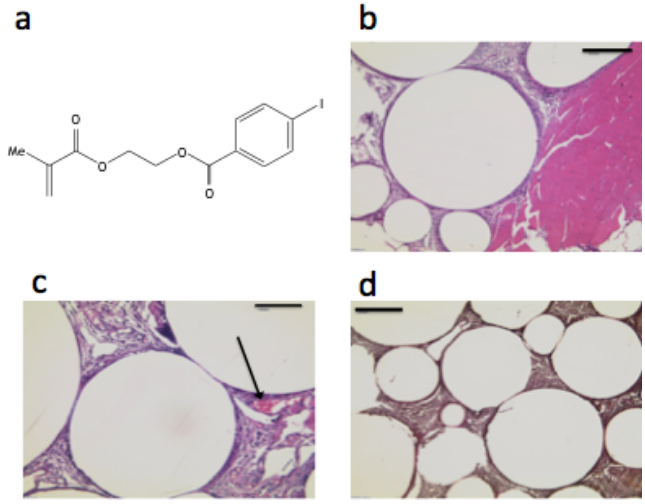

Figure 1: (a) Structural formula of the reactive monomer that is used in the manufacture of the radiopaque emblic microspheres. Note the methacryl moiety on the left side of the formula, and the aromatic ring with the covalently bound iodine. (b) Light microscopy of implanted microspheres + surrounding tissue (H/E staining), after 28 days of implantation. Around the microspheres, a mild inflammatory reaction is observed. Histiocytes have accumulated at the surface of the microspheres, especially in regions where there is no direct contact between the particles and the surrounding muscular tissue (bar = 200 µm). (c) As (b), but now at slightly larger magnification. Invaded histiocytes are clearly visible. The arrow points at a capillary blood vessel (filled with erythrocytes), which has formed to perfuse the newly formed tissue (bar = 100 µm). (d) As (b) and (c), while Elastin-van Gieson's stain was used. Note the formation of a thin collagenous capsule around most of the microspheres. This is a minimal fibrotic response, showing that the particles are well accepted in the host tissue (bar = 200 µm).

Here, we describe the essential features of our radiopaque microspheres: (i), *in vivo* biocompatibility, and (ii), X-ray imaging, both under realistic preclinical experimental conditions, and in a particular clinical situation. We also report briefly that this work provides an example of successful translation of research: the new radiopaque microspheres provided the basis for a new CE-certified medical device (class IIB) for embolization, which is now commercially available throughout Europe.

Materials and Methods

Injectability and X-ray imaging

Both kidneys were explanted from a cadaver of a rabbit that was sacrificed in a completely different experiment. The explantation was done within 20 min after sacrifice. The renal artery was prepared free, and the tip of a 20-G needle was inserted carefully into the arterial lumen. The kidneys were first flushed with saline. Then, a suspension of the microspheres (diameter range 400-600 micrometer, 20 mg microspheres in 1.6 ml) was carefully injected. The microspheres were carried along with the injection fluid, into the vascular tree of both kidneys. The kidneys were immediately frozen (-20°C) and stored until X-ray imaging. Images were recorded on a Phoenix Nanomex Imaging System (manufactured by General Electric).

In vivo biocompatibility study

This was performed by BSL BIOSERVICE Scientific Laboratories GmbH, Planegg, Germany. This company is certified according to the Principles of Good Laboratory Practice and accredited according to 90/385/EWG 93/42/EWG, and DIN EN ISO/IEC 17025:2005. The study complies with internationally accepted guidelines and recommendations regarding biological testing of medical devices:

- ISO 10993-1:2009 "Evaluation and testing within a risk management process"
- ISO 10993-6:2007 "Tests for local effects after implantation"
- ISO 10993-12:2007 "Sample preparation and reference materials":
- USP Biological Reactivity Tests, *In Vivo*, Implantation Test, current version
- OECD Series on principles of Good Laboratory Practice and compliance monitoring. Document No 13 ENV/JM/MONO (2002) [9].

Nine animals (healthy female New Zealand White Rabbits) were used (three animals per time point, i.e. 7 days, 14 days and 28 days). The rabbits were purchased from Charles River Deutschland (97633 Sulzfeld, Germany). The animals were derived from a controlled full-barrier maintained breeding system (SPF). The animals were bred for experimental purposes, according to Art. 9.2(no. 7) of the German Act on Animal welfare [26].

USP reference standard high-density poly(ethylene) (Promochem GmbH, lot no. 046) was used as the negative control material. The control samples were prepared according to the guideline ISO 10993-6, i.e. the material (film with thickness 1.0 mm) was processed by heating in a validated autoclave (121°C, 20 min). Then, the samples were cut out of the film (circular, 10 mm diameter, volume approximately 80 µL). The test samples were radiopaque iodine-containing microspheres in the diameter range 200-800 micrometer. These particles were also processed by heating in the autoclave (vide supra). In all cases, the

trocar was filled up with a quantity of microspheres corresponding to approximately 80 µl. Pre- and post-surgery; the animals were housed in an air-conditioned room. An adequate acclimatization time of at least 5 days was maintained. The animals were housed in ABS-plastic rabbit cages with a floor surface of 4200 cm^2. The temperature was 18 ± 3°C, and the relative humidity was 55 ± 10 %. The artificial light was automatically switched on and off; 12 h light and 12 h dark. The air exchange was 10 x per hour at least. The animals had free access to autoclaved hay and to Altromin 2123 (maintenance diet for rabbits, which is rich in crude fibre). The animals also had free access to tap water (drinking water, municipal residue control, microbiological controls at regular intervals). The animals were anaesthetized with ketamine (Pharmanovo, lot no. 23116, exp. Date 07/2012), and xylazine (Riemser, lot no. 000660/1, exp. Date 12/2011). The fur on the back of the test animals was shaved on both sides of the spinal column. Care was taken to avoid mechanical irritation and trauma. Then, the implantation area was washed with antiseptic solution. The test items and control material were implanted into the muscular tissue, approximately 2.5 cm. away from the midline, and approximately 2.5 cm. apart from each other. The test items were implanted on the left side of the spinal columns, the control items in the right side. A sufficient number of implant sites was used to yield 10 test specimens and 10 control specimens for assessment. The implantation period was either 7 days, 14 days, or 28 days. Post-implantation, the animals were observed at least once daily. At the end of each experimental period, the animals were euthanized with an overdose of anaesthetic. After examination and macroscopic evaluation, the test and control material implant sites were excised together with sufficient unaffected tissue, to enable the evaluation of the biological response. The tissues were fixed in a 10 % formalin-buffered solution.

Tissue samples were received by BMP Laboratory for Medical Material Testing GmbH (Aachen, Germany). This company is accredited by the Zentralstelle der Lander fur Gesundheitsschutz bei Arzneimitteln und Medizinprodukten ZLG-P-585.00.08). The samples were first cut in three equal parts, and each part was placed in a HistoTec box. The samples were dehydrated in alcohol, and then embedded in paraffin. In total, 90 samples were processed in this way: (15 control samples + 15 test samples) * 3 parts per samples. Sections of each specimen (thickness 4 µm) were cut (microtome), and stained with either hematoxylin and eosin (H&E) or Elastica von Gieson (EvG).

Results and Discussion

In vivo biocompatibility

Photomicrographs of microspheres and surrounding muscular tissue are shown in Figure 1b-1d (follow-up 28 days); the embedded microspheres appear as circular regions. Figure 1b shows the mild foreign-body reaction that is observed at the interface of the microspheres and the host tissue. There is some accumulation of histiocytes, T-lymphocytes and some foreign-body giant cells. Connective tissue formation was minimal with some collagen fibers and fibrocytes around each microsphere. Almost no fibrotic reactions were encountered, and no granulocytes or plasma cells were found. The tissue reactions are similar to those observed after 7 days or 14 days of implantation, with one exception: the density of capillaries was larger after 28 days, compared to 7-days and 14-days follow-up. This reflects the flexible and slightly compressible nature of the particles, *in vivo*. Figure 1c is a photomicrograph of the same slide, now at larger magnification. Cells and fibrotic tissue surrounding the microspheres are clearly seen. In addition, a capillary blood vessel, filled with erythrocytes (arrow) is noted. The formation of capillaries reveals that the microspheres became integrated in the host tissue. Microspheres that are in contact with each other may deform slightly, as is seen in Figure 1b and 1c. Figure 1d shows a representative photomicrograph of a similar tissue sample; this slide was treated with a mixture of picric acid and fuchsin (van Gieson's stain), which stains elastic fibers black, and collagen fibers dark-red. The very thin collagen layer around some of the microspheres shows that only a minimal encapsulation response has occurred [27].

Ex vivo embolization

"Artificial embolization" was achieved with two freshly explanted rabbit kidneys. These were perfused, via the renal artery, with a 1.8 ml of a suspension of the radiopaque microspheres (20 mg microspheres, diameter range 400-600 µm). Immediately thereafter, the kidneys were frozen and stored until X-ray imaging (Figure 2a). This revealed how the microspheres were distributed throughout the vascular beds (Figure 2b). Most of the microspheres are aligned in one of the major arteries, while other microspheres entered side branches. The data provide an example of non-specific embolization.

Preclinical *in vivo* embolization

Catheter-based embolization of the left kidneys of two living sheep was performed by an experienced interventional radiologist. Both procedures proceeded smoothly. Figure 3a shows a kidney upon perfusion with contrast, but prior to the injection of microspheres. Note that Figure 3a is a digital subtraction image, i.e. it is the difference between the X-ray images before and shortly after (several seconds) injection of contrast [25]. Hence, the image only provides information about the distribution of the injected contrast fluid; all other X-ray absorbing parts of the body are, in fact, eliminated. Numerous arterial branches within the kidney are seen clearly. The organ's contour is clearly visible as well, and this reveals that the contrast nicely flows throughout the entire organ. Figure 3b is technically the same, although this image was recorded near the endpoint of the embolization procedure. Note that Figure 3a and 3b are markedly different. In Figure 3b, the contrast is seen to accumulate in the larger arteries. The contrast hardly reaches the cortical regions of the kidney, and the organ's contour is almost invisible now. Furthermore, many small arteries are not discernable in Figure 3b. Apparently, these are no longer perfused with contrast fluid, indicating that embolization was successful.

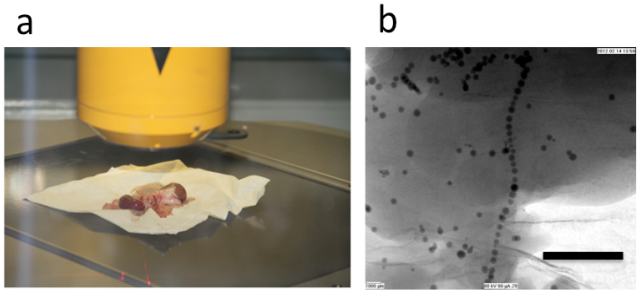

Figure 2: (a) Frozen explanted rabbit kidney, photographed during X-ray imaging in the Nanomex X-ray imaging instrument. The kidneys were explanted immediately after sacrifice of the animal, and immediately perfused, via the renal artery, with a suspension of the embolic microspheres (diameter range 400-600 µm; 1.8 ml, 20 mg microspheres). The organs containing the microspheres were frozen and stored until imaging was performed. (b) Representative X-ray image (shadow), showing the distribution of the radiopaque microspheres throughout the kidney's arterial vessel bed. Bar=5000 µm.

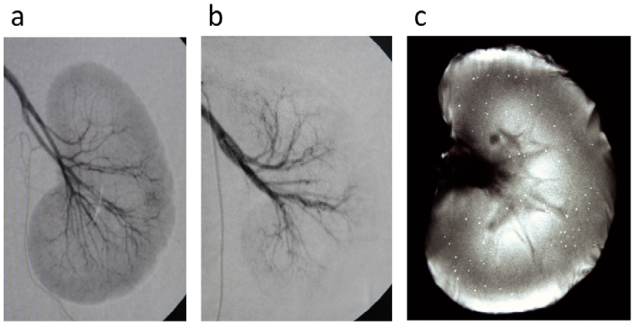

Figure 3: X-ray images, obtained during and after the embolization of the left kidney in a living sheep model. (a) Digital subtraction X-ray image of the sheep's left kidney, recorded prior to embolization. The vasculature is visible in detail; even small arteries near the organ's cortex can be discerned. (b) Same image as (a), but now recorded near the end-point of embolization. Perfusion of contrast is diminished clearly, and many small arteries are no longer seen. Dotted X-ray absorbing patterns are noted, which can possibly be ascribed to accumulated radiopaque embolic microspheres. (c) Slice abstracted from the 3D computed tomography image of the explanted embolized sheep kidney (thickness 2 mm). The radiopaque particles are seen clearly, as white dots. Note that most of the particles are found close to the cortex, where they became arrested due to gradual narrowing of the arterial branches in the kidney's arterial vessel tree.

Another striking feature seen in Figure 3b is the dotted appearance of contrast, particular in pre-cortical regions. We assume that these dots represent the radiopaque embolizing particles. We could not prove this unambiguously, given the limited sensitivity and spatial resolution that could be obtained with the imaging equipment in the animal clinic. The embolized kidneys were explanted from the animals, immediately after sacrifice. The organs were frozen, with the aim to examine them later via X-ray 3D computed tomography at higher spatial resolution. These measurements showed the embolic particles *in situ*; Figure 3c shows a horizontal slice (thickness 2 mm), which was abstracted from the data set. This image, which is representative for the entire data set, represents the center of one of the left kidneys. Note that there is no X-ray contrast fluid in the arteries any more. In Figure 3c, the microspheres are clearly visible as white (X-ray absorbing) small dots. Most of the microspheres became arrested near the cortex of the kidney [28,29]. This nicely confirms the common view, that embolic particles are carried along with the blood stream after leaving the catheter's mouth, to become arrested downstream in the arterial tree, once the diameter of the arterial branch becomes equal to their diameter (which is, in this case, in the range 400-600 μm, vide supra).

Conclusions

The new iodine-containing polymethacrylate crosslinked radiopaque microspheres are suitable for use in clinical embolization procedures. There are no concerns regarding injectability, biocompatibility or stability *in situ*. The new microspheres provide a level of X-ray visibility that-in principle-allows the interventional radiologist to localize the embolic particles during and after the embolization procedures. The extent of "visibility" depends on several factors, such as: spatial distribution of the microspheres, diameter size of the microspheres (for small- sized microspheres only ensembles of the particles will be detectable), proximity of bone tissue, quality of the X-ray imaging equipment, etc.). The idea that the use of X-ray visible embolic particles may translate into advantages for patients, clinicians and heath care systems is clearly growing stronger [24-26]. It is, however, still unclear for which type of embolizations the feature will be most advantageous. We anticipate that the feature will be particularly helpful in pre-operative embolization of cerebral tumors, which can be done to prevent bleeding complications during surgery. Monitoring of the embolic particles may help to prevent non-target embolization, and can help to judge whether or not total embolization has been achieved. The latter is important to maximize the chances for success. The new radiopaque microspheres are used in a new CE-certified medical device for embolization, called X-Spheres. Therefore, this work provides a quite unusual example of translational development of a new medical device, classified within the highest-but-one risk group (IIB), on the basis of a new synthetic polymer biomaterial that was originally developed in an academic laboratory.

Competing Interests

The authors Y.B.A. and L.H.K. declare to have stock in the company Interface BIOmaterials BV (Geleen, The Netherlands). This company is the manufacturer of the new embolization product X-Spheres; this product utilizes radiopaque embolic microspheres.

Acknowledgements

We thank Dr. U. Mueller, Professor B. Klosterhalfen and mr. C. Musters for advice and technical assistance. We thanks prof. P. Lohle (Elisabeth Hospital Tilburg, the Netherlands) for performing the kidney embolizations in the sheep models. This study was financed, in part, by the Interreg IV-A project 'BioMiMedics' (www.biomimedics.org) (Interreg IV-A 1.2-2010-03/063). The Universities of Maastricht, Liege (Belgium), Hasselt (Belgium) and Aachen (Germany; RWTH and Fachhochschule), as well as several local regional biotechnological enterprises cooperated in 'BioMiMedics'. This particular study was financed through generous contributions of the EU (through INterreg IV-A), the Government of the Province Dutch Limburg, the Dutch National Ministry of Economic Affairs, Agriculture and Innovation, Maastricht University, The Limburg Bank for Industry Innovation (LIOF), and the Company INterface BIOmaterials BV (Geleen, The Netherlands).

References

1. Iqbal J, Gunn J, Serruys PW (2013) Coronary stents: Historical development, current status and future directions. Br Med Bull 106: 193-211.
2. Sternberg K, Grabow N, Petersen S, Weitschies W, Harder C, et al. (2013) Advances in coronary stent technology--active drug-loaded stent surfaces for prevention of restenosis and improvement of biocompatibility. Curr Pharm Biotechnol 14: 76-90.
3. Nikam N, Steinberg TB, Steinberg DH (2014) Advances in stent technologies and their effect on clinical efficacy and safety. Med Devices (Auckl) 7: 165-178.
4. Garg S, Bourantas C, Serruys PW (2013) New concepts in the design of drug-eluting coronary stents. Nat Rev Cardiol 10: 248-260.
5. Brugaletta S, Garcia-Garcia HM, Onuma Y, Serruys PW (2012) Everolimus-eluting ABSORB bioresorbable vascular scaffold: present and future perspectives. Expert Rev Med Devices 9: 327-338.
6. Khan AT, Shehmar M, Gupta JK (2014) Uterine fibroids: current perspectives. Int J Womens Health 6: 95-114.
7. Spies JB (2013) Current evidence on uterine embolization for fibroids. Semin Intervent Radiol 30: 340-346.
8. Lopera J, Suri R, Kroma GM, Garza-Berlanga A, Thomas J (2013) Role of interventional procedures in obstetrics/gynecology. Radiol Clin North Am 51: 1049-1066.
9. Bulman JC, Ascher SM, Spies JB (2012) Current concepts in uterine fibroid embolization. Radiographics 32: 1735-1750.
10. Van der Kooij SM, Ankum WM, Hehenkamp WJ (2012) Review of nonsurgical/minimally invasive treatments for uterine fibroids. Curr Opin Obstet Gynecol 24: 368-375.
11. Salazar GM, Petrozza JC, Walker TG (2009) Transcatheter endovascular techniques for management of obstetrical and gynecologic emergencies. Tech Vasc Interv Radiol 12: 139-147.
12. Van der Kooij SM, Bipat S, Hehenkamp WJ, Ankum WM, Reekers JA (2010) Uterine artery embolization vs hysterectomy in the treatment of symptomatic

uterine fibroids: 5-year outcome from the randomized EMMY trial. Am J Obstet Gynecol 203: 105 e1-e13.

13. Van der Kooij SM, Hehenkamp WJ, Birnie E, Ankum WM, Mol BW, et al. (2013) The effect of treatment preference and treatment allocation on patients' health-related quality of life in the randomized EMMY trial. Eur J Obstet Gynecol Reprod Biol 169: 69-74.
14. Hehenkamp WJ, Volkers NA, Birnie E, Reekers JA, Ankum WM (2006) Pain and return to daily activities after uterine artery embolization and hysterectomy in the treatment of symptomatic uterine fibroids: results from the randomized EMMY trial. Cardiovasc Intervent Radiol 29: 179-187.
15. Hehenkamp WJ, Volkers NA, Donderwinkel PF, De Blok S, Birnie E, et al. (2005) Uterine artery embolization versus hysterectomy in the treatment of symptomatic uterine fibroids (EMMY trial): peri- and postprocedural results from a randomized controlled trial. Am J Obstet Gynecol 193: 1618-1629.
16. Pisco JM, Duarte M, Bilhim T, Cirurgião F, Oliveira AG (2011) Pregnancy after uterine fibroid embolization. Fertil Steril 95: 1121-1126.
17. Pinto Pabón I, Magret JP, Unzurrunzaga EA, García IM, Catalán IB, et al. (2008) Pregnancy after uterine fibroid embolization: follow-up of 100 patients embolized using tris-acryl gelatin microspheres. Fertil Steril 90: 2356-2360.
18. Torre A, Paillusson B, Fain V, Labauge P, Pelage JP, et al. (2014) Uterine artery embolization for severe symptomatic fibroids: effects on fertility and symptoms. Hum Reprod 29: 490-501.
19. Saralidze K, Van Hooy-Corstjens CS, Koole LH, Knetsch ML (2007) New acrylic microspheres for arterial embolization: combining radiopacity for precise localization with immobilized thrombin to trigger local blood coagulation. Biomaterials 28: 2457-2464.
20. Saralidze K, Knetsch ML, Van der Marel C, Koole LH (2010) Versatile polymer microspheres for injection therapy: aspects of fluoroscopic traceability and biofunctionalization. Biomacromolecules 11: 3556-3562.
21. Sharma KV, Dreher MR, Tang Y, Pritchard W, Chiesa OA, et al. (2010) Development of "imageable" beads for transcatheter embolotherapy. J Vasc Interv Radiol 21: 865-876.
22. Galperin A, Margel S (2006) Synthesis and characterization of new micrometer-sized radiopaque polymeric particles of narrow size distribution by a single-step swelling of uniform polystyrene template microspheres for X-ray imaging applications. Biomacromolecules 7: 2650-2660.
23. Stampfl U, Sommer CM, Bellemann N, Holzschuh M, Kueller A, et al. (2012) Multimodal visibility of a modified polyzene-F-coated spherical embolic agent for liver embolization: Feasibility study in a porcine model. J Vasc Interv Radiol 23: 1225-1231.
24. Duran R, Sharma K, Dreher MR, Ashrafi K, Mirpour S, et al. (2016) A novel inherently radiopaque bead for transarterial embolization to treat liver cancer -a preclinical study. Theranostics 6: 28-39.
25. Tacher V, Duran R, Lin M, Sohn JH, Sharma KV, et al. (2015) Multimodality imaging of ethiodized oil-loaded radiopaque microspheres during transarterial embolization of rabbits with VX2 liver tumors. Radiology 16: 141624.
26. Johnson CG, Tang Y, Beck A, Dreher MR, Woods DL, et al. (2016) Preparation of radiopaque drug-eluting beads for transcatheter chemoembolization. J Vasc Interv Radiol 27: 117-126.
27. Shlansky-Goldberg RD, Rosen MA, Mondschein JI, Stavropoulos SW, Trerotola SO, et al. (2014) Comparison of polyvinyl alcohol microspheres and tris-acryl gelatin microspheres for uterine fibroid embolization: results of a single-center randomized study. J Vasc Interv Radiol 25: 823-832.
28. Salazar GM, Petrozza JC, Walker TG (2009) Evaluation and management of acute vascular trauma. Tech Vasc Interv Radiol 12: 139-147.
29. German Animal Welfare Act (2009).